Electrode Pitting in Resistance Spot Welding of Aluminum Alloy 5182

I. LUM, S. FUKUMOTO, E. BIRO, D.R. BOOMER, and Y. ZHOU

Electrode pitting was investigated in resistance spot welding of 1.5-mm-thick sheet aluminum alloy 5182 using a medium-frequency direct-current welder and electrodes with a tip face curvature radius of 50 mm and tip face diameter of 10 mm. Detailed investigation of the metallurgical interactions between the copper electrode and aluminum alloy sheet was carried out using scanning electron microscopy/energy-dispersive X-ray spectroscopy (SEM/EDX) and X-ray diffraction (XRD). The results indicated that electrode degradation, which eventually leads to weld failure, proceeded in four basic steps: aluminum pickup, electrode alloying with aluminum, electrode tip face pitting, and cavitation. Since pitting and cavitation result from Al pickup and alloying, periodic electrode cleaning could extend electrode tip life by limiting the buildup of Al on the tip face. This work is part of the effort to improve electrode tip life in resistance spot welding of aluminum alloys for automotive applications.

I. INTRODUCTION

ALUMINUM alloys are attractive to the automotive industry because of their low density, high corrosion resistance, and recyclability. However, one of the major problems in high-volume resistance spot welding (RSW) of aluminum is short electrode tip life[1,2] compared to that of Zn-coated steels.[3] Much of the prior work performed on electrode tip life during RSW of aluminum has studied the influences of electrode design (including copper alloys,[4] coating,[5] and configuration[6]), sheet,[7,8] and electrode[9] surface conditions. However, detailed work on the mechanisms of electrode degradation during RSW of aluminum has been quite limited.[10]

It is generally agreed that copper electrodes degrade as a result of excessive pitting on the tip face during RSW of aluminum. Patrick *et al*.[11] proposed a model that includes electrode local melting, alloying, and pitting. Regular production aluminum sheets have surface oxide that is relatively thick, and, when the electrode contacts the sheet, the oxide layer fractures, creating scattered, small points for welding current conduction. When the high current is applied, it is forced through these severe current constrictions, causing excessive heating and resulting in local melting and alloying of the copper and aluminum. As the electrode is separated from the sheet, electrode pitting occurs as material is removed from the tip face. This causes rapid electrode deterioration as welding progresses. Very limited experimental research has been published to support the proposed model.[11]

Dilthey and Hicken[12] suggested that the formation of Cu-Al alloys, resulting from diffusion between the aluminum and copper, was primarily responsible for the wear of the electrodes. Electrodes were said to adhere to the aluminum sheet because of the formation of Cu-Al phases. The subsequent separation process then fractured the brittle Cu-Al phases causing a loss of material from the electrode tip. It was therefore suggested that Cu-Al phases should be removed as frequently as possible, *e.g*., by regular cleaning of the electrode tip face. The Cu-Al phases on electrode tip faces were observed by scanning electron microscopy (SEM) with energy-dispersive X-ray spectroscopy (EDX) and detected by X-ray diffraction (XRD) to be $CuAl_2$ phase after the first weld and Cu_9Al_4 after five welds, but no XRD spectra were published to support the claim. It was also suggested that the temperature at the electrode/sheet interface was in the proximity of the melting point of the copper (around 1358 K), since freely solidified surfaces were observed locally on the electrode tip faces. However, the Cu-Al phase diagram,[13] in fact, indicates that Cu-Al eutectic melting could occur at 821 K, which is much lower than the melting point of copper.

In a previous study,[14] the electrode tip life in RSW of aluminum alloy 5182 was investigated by monitoring contact areas at faying and electrode/sheet interfaces and joint shear strength based on a modified version of the MIL-W-6858D standard. The results indicated that electrode tip life, defined as the first weld number at which the joint strength dropped below 80 pct of its initial value, varied from approximately 400 to 900 welds even though all the process conditions were intentionally kept constant. Despite the large variation in electrode life, distinct patterns (Figure 1 as a typical example) were found to correlate electrode failure to electrode degradation in terms of the change in the electrode contact area (*i.e*., the area on the tip face that touched the sheet during welding).

1. Stage I: at the beginning of the electrode life, the contact area and joint strength were relatively constant.
2. Stage II: in this period, the joint strength increased and peaked. Incipient electrode pitting was observed (at about 360 welds) just before the strength peaked. The electrode contact area started to increase after the onset of electrode pitting. It was believed that the initial increase in shear strength was due to aluminum alloy pickup and alloying, and later due to the increase in electrode contact area.

I. LUM, Graduate Student, E. BIRO, Research Engineer, and Y. ZHOU, Canada Research Chair in Microjoining, are with the Department of Mechanical Engineering, University of Waterloo, Waterloo, ON, Canada N2L 3G1. Contact e-mail: nzhou@uwaterloo.ca S. FUKUMOTO, Research Associate, is with the Department of Materials Science and Engineering, Faculty of Engineering, Himeji Institute of Technology, Himeji, Hyogo, Japan 671-2201. D.R. BOOMER, Welding Specialist, is with Banbury Laboratory, Alcan International Limited, Oxfordshire, United Kingdom OX16 7SP.

Manuscript submitted December 2, 2002.

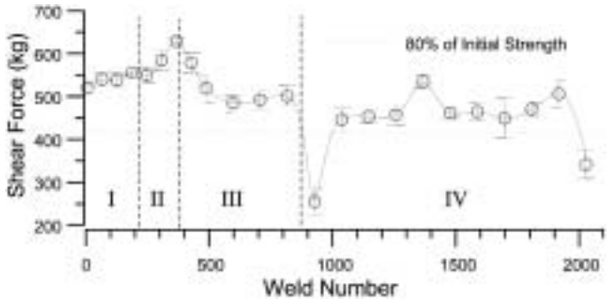

Fig. 1—The plot of joint strength *vs* weld number of a typical electrode life test.[10]

3. Stage III: the joint strength started to drop, as the contact area continued to increase because pitted areas grew and combined into large cavities, until the electrode failed (at about 920 welds). The reduction in joint strength was due to the large increase in the contact area at the sheet faying interface and hence reduction in current density and formation of an undersized weld.
4. Stage IV: after the electrode failure, the joint strength varied greatly and unpredictably as the morphology of the pitted areas changed erratically and dynamically.

This present work focuses on metallurgical aspects of the electrode pitting process in RSW of aluminum alloy 5182. Effects of periodic electrode cleaning have also been investigated in support of the study on electrode pitting mechanisms.

II. EXPERIMENTAL

Welds were made on 1.5-mm-thick, electrolytically cleaned sheet aluminum alloy AA5182-H111 (Table I) using a 170 kVA medium frequency direct current (MFDC) pedestal resistance spot welder. All tests used class I (Cu-0.15 pct Zr) electrodes with a taper angle of 60 deg, a tip face diameter of 10 mm, and radius of curvature of 50 mm (Figure 2). Before being installed on the welder, the electrode tip faces were cleaned with a Scotchbrite™ (3M, St. Paul, MN) abrasive pad until all visible surface oxide was removed. Caution was paid to ensure that the electrode tip geometry was not altered by this cleaning. No cleaning was performed on the sheet surface prior to welding. The welding schedule is shown in Table II.

To investigate the change in electrode tip face morphology, several nominally identical new electrodes were used to make a specific number of welds and then were dismounted from the welder for metallurgical analysis. It was observed that electrode degradation was more significant on top electrodes than on bottom electrodes, which is obviously due to the polarity effect since top and bottom electrodes remain positive and negative, respectively, during welding. According to the *Peltier* effect,[15] the heat generation should be higher at the top tip face than at the bottom tip face, which would cause faster electrode degradation at the top electrode. This was actually found to be the case in these experiments, and therefore, this study has considered only the behavior of the top electrodes. Cross sections of the electrodes, and electrode and sheet surfaces, were observed by SEM/EDX. Used electrode tip faces were also analyzed using XRD. To further investigate possible alloys formed on the electrode tip faces during welding, a diffusion experiment was performed, in which an unused electrode was dipped into a bath of molten AA5182 at 1123 K for 5 seconds, and then air-cooled. The tip surface with reaction

Table I. Chemical Composition of AA5182

Element	Si	Fe	Cu	Mn	Mg	Al
Mass pct	0.08	0.19	0.05	0.32	4.71	bal

Table II. Welding Schedule

Squeeze	25 cycles
Weld time	5 cycles
Hold time	12 cycles
Weld force	6 kN
Current	29 kA
Welding rate	20/min

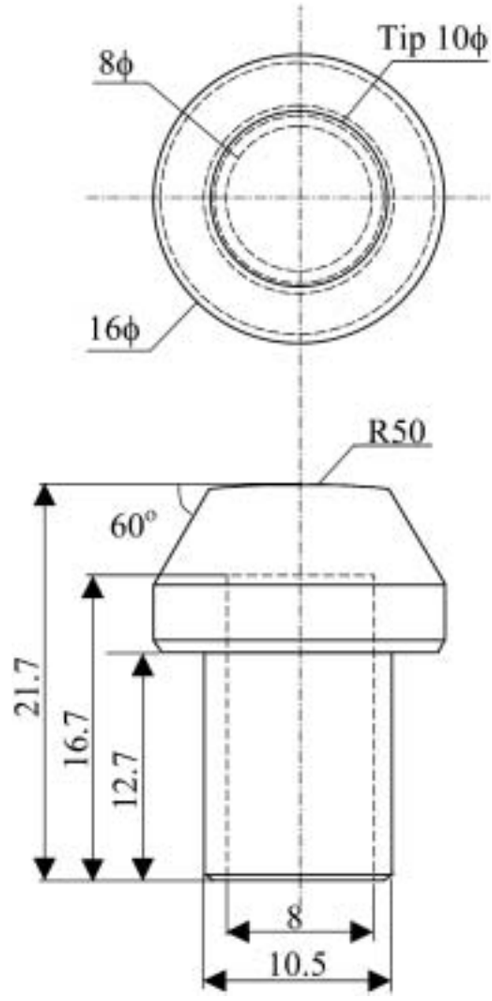

Fig. 2—Configuration of the electrode (unit: mm).

layer developed in the diffusion experiment was analyzed using XRD. The selection of 1123 K is rather arbitrarily set at 200 to 300 K above the melting point of AA5182.

In electrode tip life tests, the sample welds were periodically evaluated by shear testing, in which 10 pct of the welds were tested up to 500 welds, and 5 pct were tested after 500 welds. Electrode tip life was defined as the first weld number when the shear strength dropped below 80 pct of its initial value. Further details on the procedure used for the life test can be found in the previous study.[14] In the present study, two sets of life tests were also conducted where the tip faces of both top and bottom electrodes were periodically manually cleaned at intervals of 20 or 50 welds with a Scotchbrite™ flap wheel mounted on an electric drill. The intent of cleaning was to remove aluminum alloy picked up on the surface of the electrode without significantly changing the tip geometry. The cleaning direction was rotated 90 deg for each successive cleaning, in order to balance the material removal and minimize the change in the surface geometry. After the cleaning operation, compressed air was used to remove debris from the electrode surface.

III. RESULTS AND DISCUSSION

A. *Electrode Tip Face Morphology*

Figure 3 shows optical photographs of electrode tip surfaces that were used for different specific numbers of welds. Figure 4 shows the carbon imprints taken from the same electrode tips immediately before the electrodes were dismounted from the welder.

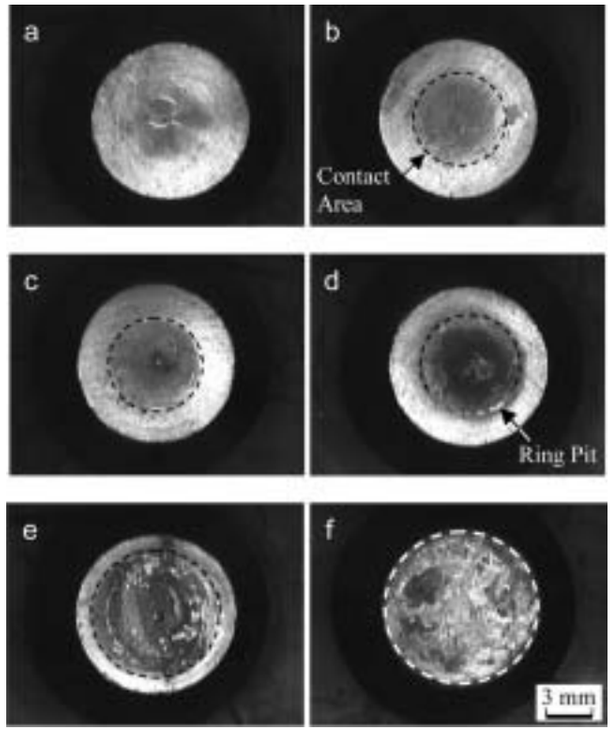

Fig. 3—Electrode surfaces after (*a*) 20, (*b*) 50, (*c*) 100, (*d*) 200, (*e*) 500, and (*f*) 2000 welds. The contact area is shown in dashed lines.

Prior to starting welding, the electrode tip faces were clean and without visual blemishes. Soon after welding began, the electrode contact areas (*i.e.*, the area that touched the sheet during welding) started to turn a dull gray, as seen in Figure 3. The color change was macroscopic visual evidence of the widespread aluminum alloy pickup found on the electrodes.

Further and more detailed study of this effect will be reported in this article. At about 200 welds, the first visual evidence of pitting could be seen on the contact area with the naked eye (Figure 3(d)), and the same effect was also clearly shown on the carbon imprints (Figure 4(d)). The first pitting occurred at the peripheral region and these pits soon formed a ring pattern around the contact area (Figure 3(d)). Once the ring of pits was fully formed, it extended toward the center of the tip face and subsequently formed a large cavity in the center of the electrode (Figures 3(e) and (f) and 4(e) and (f)). The contact area started to increase after the onset of electrode pitting (Figures 3 and 4). The electrode failed when the increase in the contact area at the faying interface was above a certain threshold at which the resultant current density was too low, resulting in undersized welds.[14]

In the following Sections B and C, investigation of the metallurgical interaction between electrodes and aluminum

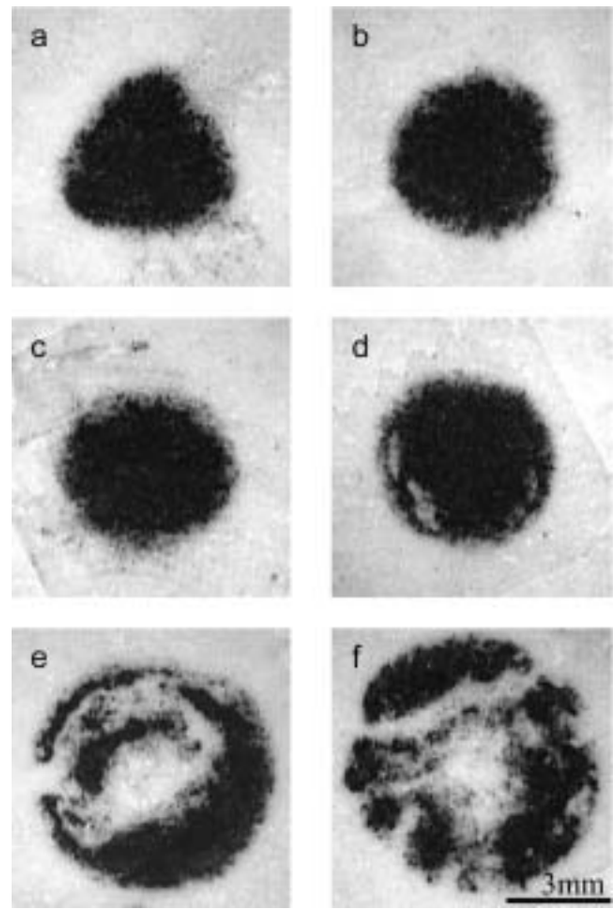

Fig. 4—Electrode carbon imprints corresponding to the contact areas in Figure 3: (*a*) 20, (*b*) 50, (*c*) 100, (*d*) 200, (*e*) 500, and (*f*) 2000 welds.

alloy sheets (such as pickup, alloying, electrode pitting, and cavitation) will be described in detail.

B. *Pickup and Alloying*

Figure 5(a) shows a particle of foreign material on the electrode tip surface after the first weld. This material was identified with EDX analysis to be 96 mass pct Al-4 mass pct Mg, which is approximately the same composition as the sheet aluminum alloy (Table I). Therefore, the pickup of aluminum alloy by the electrodes even started at the first weld. An Al alloy sphere was also observed on the aluminum alloy sheet surface after the first weld (Figure 5(b)), which is believed to result from molten aluminum produced during welding. As Patrick *et al.*[11] suggested, the current constrictions during welding, created by the fractures of the surface oxides, would result in a very high current density and hence local aluminum melting. This molten Al would wet and result in Al pickup on the electrode tip face. The Al pickup was quantified by periodic examination of the electrode contact area with EDX. As can be seen in Table III, the Al content increased as a function of weld number to a maximum of about 64 pct. The thickness of eutectic and alloying layers varied from a few up to 30 μm. Afterward, the Al content of the face varied as the electrode pitted and refilled/recoated with fresh Al alloy.

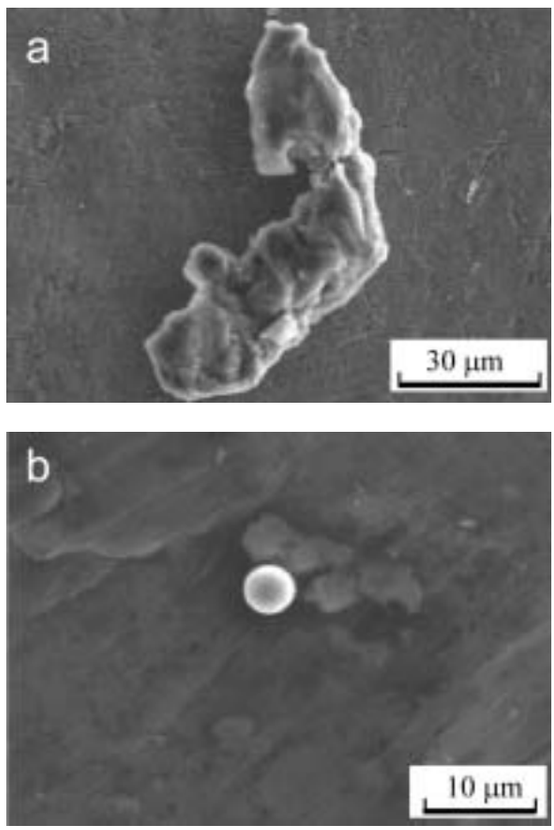

Fig. 5—(*a*) Al alloy pickup on electrode after the first weld and (*b*) Al alloy sphere on aluminum sheet.

Once the Al was picked up on the electrode tip face, the electrode alloyed with the Al. Figure 6 shows one of the local, alloyed regions from a cross section of an electrode, after making 200 welds. The EDX analysis was performed to estimate compositions of possible Cu-Al phases (Table IV) as compared to those of the equilibrium Cu-Al phases (Table V).[13] Solidification structure is clearly shown in Figure 6, which may be the eutectic with the bright network of $CuAl_2$ and the darker regions of Al(Cu) solid solution. The solidification structure further confirmed that melting occurred during welding. Another alloy layer, possibly Cu_9Al_4, was also observed between the possible $CuAl_2$ layer and electrode base metal (E in Figure 6(b)).

Table III. Al Content Measured on Electrode Tip Face

Weld Number	Aluminum Content on Electrode Face (Mass Pct)
20	0.9
50	12.3
100	24.2
200	63.6
500	39.0
2000	57.5

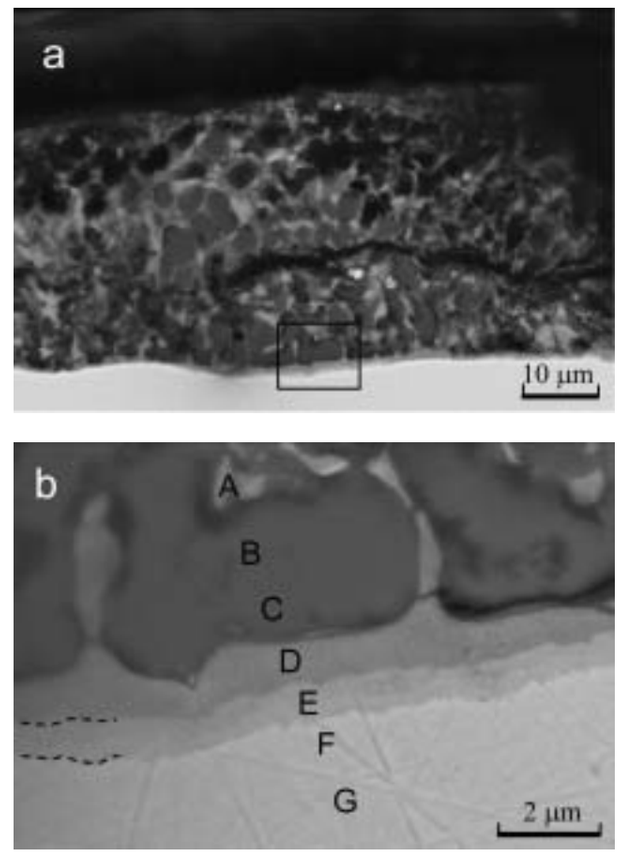

Fig. 6—Cross section of an electrode after 200 welds showing (*a*) solidified alloy layer and (*b*) higher magnification of highlighted area in (a). The compositions at various locations are listed in Table IV.

Table IV. Chemical Composition Estimated Using EDX in Figure 6

Location	Cu (Mass Pct)	Al (Mass Pct)	Mg (Mass Pct)	Possible Phase
A	48.5	51.1	0.4	$CuAl_2$
B	26.8	73.0	0.2	Al(Cu)
C	30.2	69.7	0.1	Al(Cu)
D	66.0	33.9	0.1	$CuAl_2$
E	81.0	19.0	0	Cu_9Al_4
F	98.8	1.2	0	Cu(Al)
G	100	0	0	Cu(Al)

Table V. Composition of Major Equilibrium Phases in the Al-Cu System[13]

Equilibrium Phase	Cu (Mass Pct)	Maximum Melting (or Transformation) Temperature (K)
Al(Cu)	0 to 5.7	933
Cu Al_2	52.4 to 53.7	863
Cu_9Al_4	79.9 to 84.0	1046 ($\gamma_1 \leftrightarrow \gamma_0 + \varepsilon_1$)
Cu(Al)	90.6 to 100	1358

The XRD analysis was performed on the tip face of an electrode after making 2000 welds, and also on the sample surface from the diffusion experiment (Figure 7). Although the existence of $CuAl_2$ and Cu_9Al_4 on the tip face of the welded electrode is inconclusive from the XRD analysis, $CuAl_2$ was clearly identified on the diffusion sample (Figure 7(b)). The total amount of intermetallic phases may be too small to be detected on a welded electrode since the alloyed layers were generally very thin and only in local spots. Dilthey and Hicken[12] reported finding $CuAl_2$ even after the first weld and Cu_9Al_4 after five welds but did not present any XRD data. Cu-Al intermetallic phases (mainly $CuAl_2$ and Cu_9Al_4) were observed by XRD in the interfacial regions of both diffusion-bonded and roll-bonded aluminum and copper joints,[16,17] in which a large amount of intermetallic phases could easily form because of the longer time experienced at elevated temperatures (a few hours). In RSW, very short weld time (much less than 1 second) and repeated pitting (removal of alloyed layers) would limit the formation and accumulation of intermetallic phases. Another difference in RSW is that the reaction between solid copper and molten aluminum would indicate a larger amount of $CuAl_2$ phase because of the eutectic reaction and Cu_9Al_4 would only form through solid diffusion between the $CuAl_2$ phase and the copper base metal, which is limited by the short weld duration. This may explain why only traces of possible Cu_9Al_4 were observed.

It was suggested that Al pickup and alloying with the electrode tip face was responsible for the initial increase in joint strength, since the resultant increase in contact resistance would increase heat generation for nugget formation.[10]

C. *Pitting and Cavitation*

As already pointed out by others,[11,12] electrode pitting is a result of material removal from the electrode tip face. Two pitting mechanisms were noted in this study, which will be illustrated as follows from a number of small pits that formed

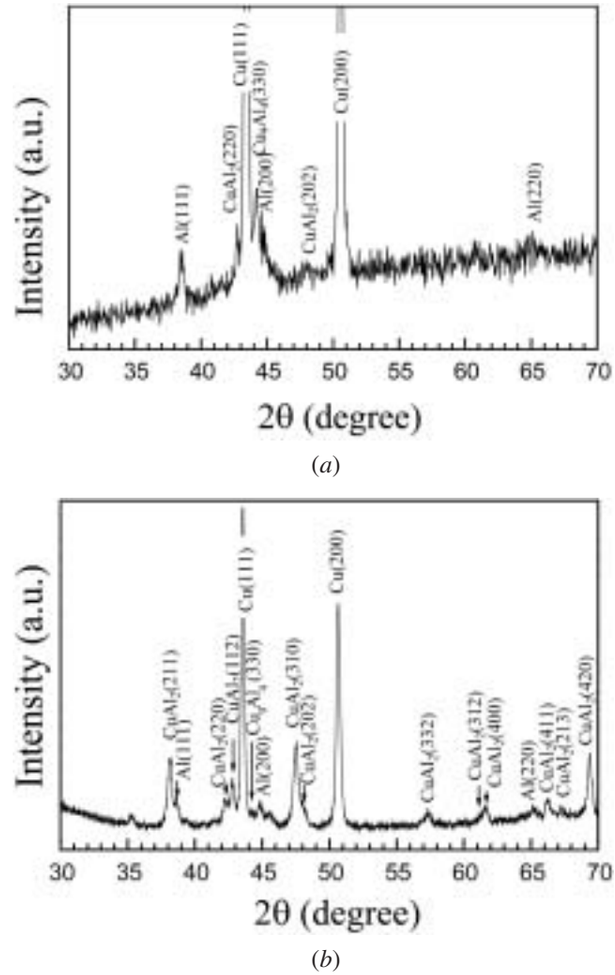

Fig. 7—XRD spectra of (*a*) electrode tip face after 2000 welds and (*b*) diffusion experiment sample.

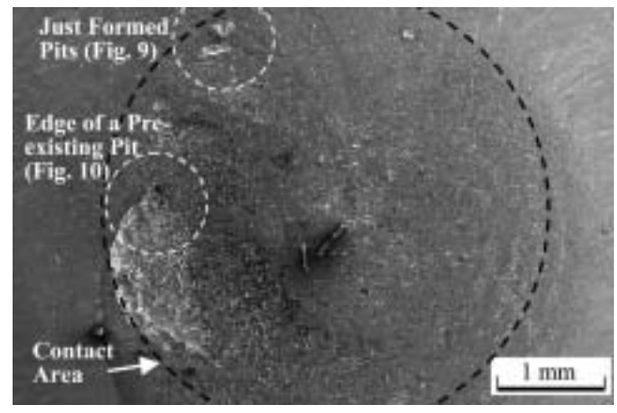

Fig. 8—Pitting at the edge of the contact area on an electrode after 96 welds.

at the edge regions of the contact area of an electrode after making 96 welds (Figure 8).

First, electrode pitting occurred by brittle fracture of local bonds (intermetallic phases) formed between the electrode

tip face and sheet surface resulting in material removal from the electrode tip face. Figure 9 shows two pits formed in this manner, in which two foreign particles on the Al alloy sheet match the pits on the electrode. In other words, the electrode pits formed as a result of the particles removed from the electrode tip face. The relatively flat features (*i.e.*, lack of deformation) of the fractures indicate that the two particles were pulled away from the electrode in a brittle manner. The EDX analysis indicated that the particles on the Al alloy sheet were 54 mass pct Cu-46 mass pct Al (33 at. pct Cu-66 at. pct Al), the approximate composition of $CuAl_2$. It is also interesting to note that the fractured areas at the edge of the electrode pits were rich in Al (Figure 9(b)), which suggests that fracturing occurred through brittle Cu-Al phase(s). Cracks in Cu-Al phase(s) also can be seen in Figure 6(a). This type of pitting mechanism is similar to that proposed by Dilthey and Hicken.[12]

Second, electrode pitting also occurred by local melting of the electrode tip face, resulting in molten material transfer onto the sheet surface. Figure 10 shows a re-solidified Cu-rich particle on the Al alloy sheet, which matches a pit formed on the corresponding electrode surface. Solidification structure was also observed on the pit surface (Figure 10), which further confirms that the particle on the sheet separated from the electrode when it was still molten. The EDX analysis showed that the pit area on the electrode was 86 mass pct Cu-14 mass pct Al (72 at. pct Cu-28 at. pct Cu), which may suggest the existence of Cu_9Al_4 underneath the pit surface. It is worth noting that this pit was found inside a pre-existing, much larger pitted region. It is believed that during welding the temperature experienced in this region was very high due to the poor contact and hence higher contact resistance, and melting and further alloying occurred. When the electrode pulled away from the sheet after welding, this entire region was still molten, resulting in part of the molten alloy depositing onto the sheet. This is further confirmed by the dendritelike protrusions surrounding the small pit within the pre-existing pitted region (Figure 10). This type of pitting mechanism has not previously been reported in the literature.

Once pitting started, cavities formed by combining smaller pits. Figure 11 shows part of a sheet surface after 76 and 77 welds and the corresponding electrode tip face after 85 welds. Three islands of material transfer were on the sheet surface after 76 welds (Figure 11(a)). On the subsequent weld, the three islands have combined to form a larger pit, and a new island adjacent to the larger pit formed as well (Figure 11(b)). Upon examination of the electrode tip face (Figure 11(d)), it can be seen that the pit, A′, has taken the shape of an agglomerated area, A, on the sheet surface at weld 77.

The Al content on the electrode tip face is determined by Al alloy pickup and Cu-Al material loss from the electrode tip face. At the early stage of tip life, the Al content increased as the weld number increased (Table III), as described previously. But, after heavy pitting and cavitation started, the Al content varied as the electrode pitted and was refilled/recoated.

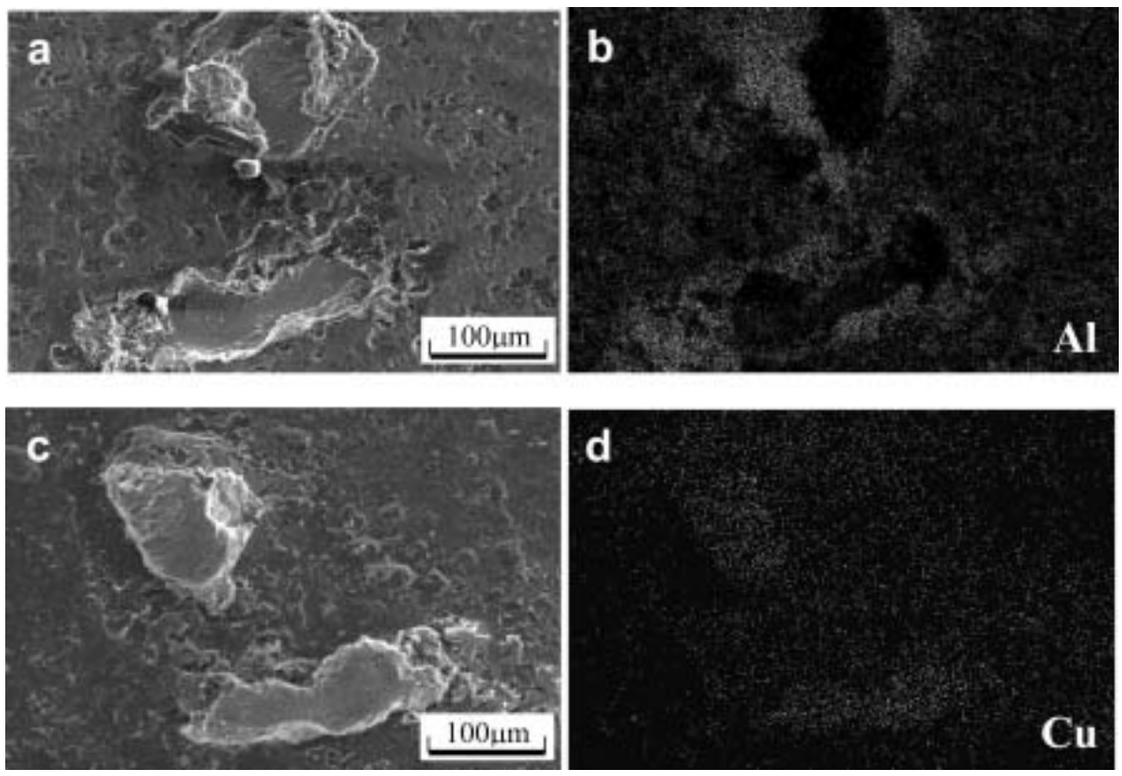

Fig. 9—Electrode pitting (Fig. 8) that occurred in solid state showing (*a*) material removal from electrode tip face, (*b*) Al mapping of (a), (*c*) corresponding material pickup on Al sheet surface, and (*d*) Cu mapping of (c).

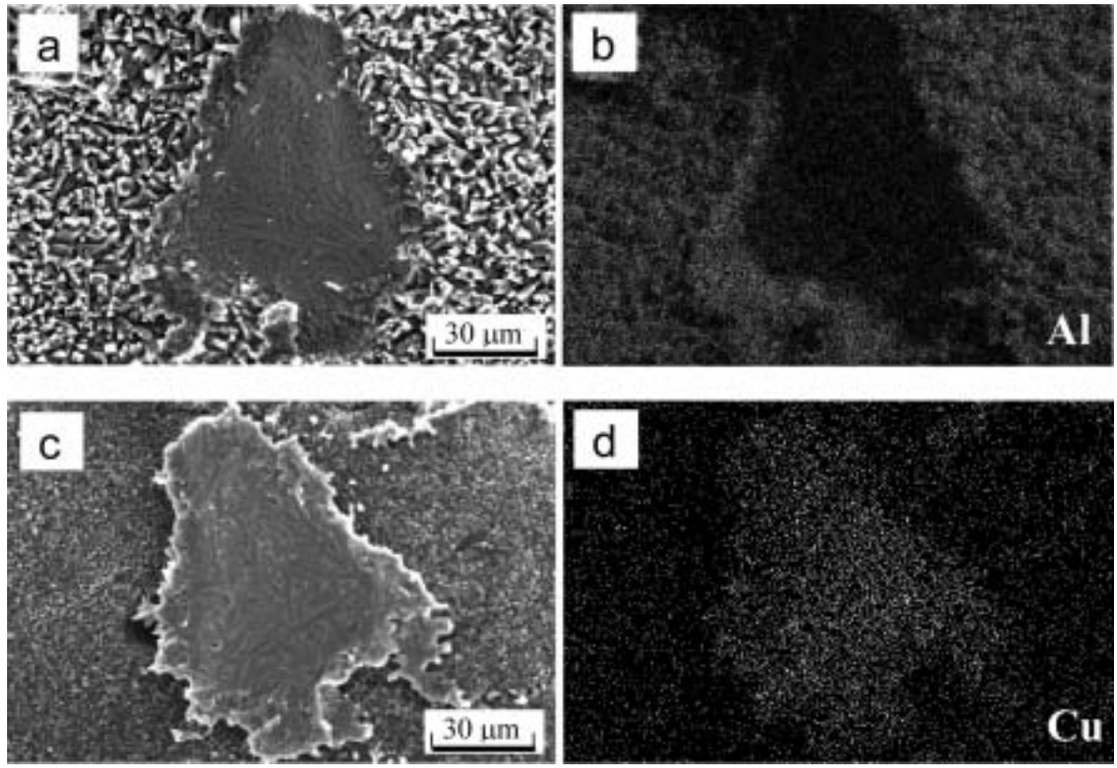

Fig. 10—Electrode pitting (Fig. 8) that occurred in molten state showing (*a*) material removal from the electrode tip face, (*b*) Al mapping of (a), (*c*) corresponding material pickup on Al sheet surface, and (*d*) Cu mapping of (c).

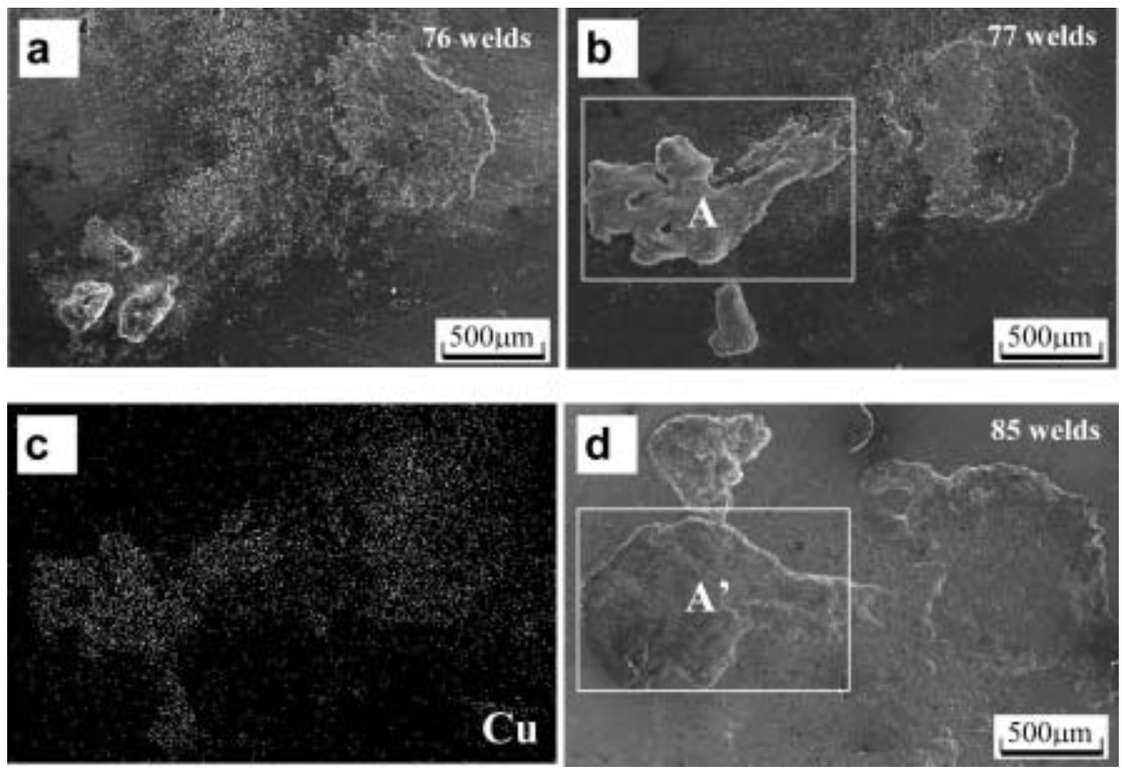

Fig. 11—Progress of pitting showing (*a*) material pickup on the Al sheet after 76 welds, (*b*) after 77 welds, (*c*) Cu mapping of (b), and (*d*) corresponding pits formed on the electrode tip face after 85 welds.

D. *Electrode Degradation*

Based on the results and discussion presented in Section C, electrode degradation, which eventually leads to weld failure, is proposed to form in four basic steps (Figure 12) during RSW of aluminum alloy 5182: aluminum alloy pickup, electrode alloying with aluminum, electrode tip face pitting, and cavitation.

Aluminum alloy pickup begins from the first weld as tiny drops of molten Al alloy are transferred from the sheet surface to the electrode tip face. Local melting occurs because of the very high current density resulting from the constriction at the points of cracked oxide layer on the sheet surface.[12] This molten Al alloy transfer would occur mostly at the edge of the contact area where the temperatures are the highest due to the concentration of current density and increasing contact resistance.[18] The molten Al alloy adheres to the surface of the Cu electrode, on which it wets better than on the Al alloy sheet because the sheet was covered by Al oxide. As molten Al alloy is transferred onto the electrode tip face, it reacts with the electrode surface forming a complex alloyed layer. This Cu-Al mixture will further increase the local resistivity and heat generation, thus increasing local melting around the alloyed regions on the tip face.

If the Cu-Al mixture is still molten when the electrode is parted from the sheet after welding, some of the molten alloy may adhere to the sheet, resulting in material removal from the electrode tip face. If the Cu-Al mixture has solidified before the electrode is separated from the sheet, brittle fracture of the Cu-Al intermetallic phase(s) will also result in material removal from the electrode tip face. Thus, pits may form by either fracturing of intermetallic phase(s) or transfer of molten Cu-Al mixture. Initial pitting occurs on a ring near the periphery of the contact area because this is where the surface temperature would be the highest. The high temperature in this region would lead to the highest rate of Al alloy pickup and hence the highest rate of alloying compared to the rest of the contact area. Once this ring is formed, pitting grows both inward and outward to form large cavities by combining smaller pitted areas. It appears that pitting first grows faster inward than outward. Once the central cavity has formed, the contact concentrates at the outside edge of the central cavity and pitting starts to grow outward.[10]

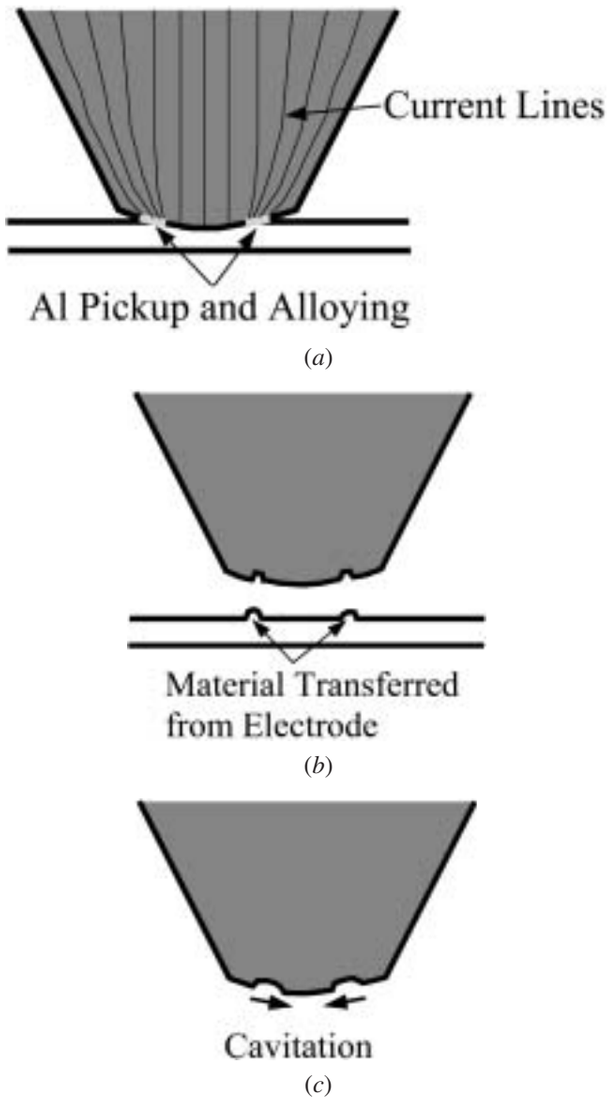

Fig. 12—Schematic of pitting process showing (*a*) Al pickup and alloying on electrode (since first weld), (*b*) pit formed as material loss from electrode (65 to 340 welds), and (*c*) pit growing to form large cavity (120 to 360 welds).

E. *Electrode Cleaning*

If pitting and cavitation are indeed the result of Al pickup and alloying, as discussed in Section D, electrode cleaning to prevent or minimize the buildup of Al should improve the electrode tip life. This was investigated in two sets of tip life tests with periodic cleaning. As expected, Figure 13 shows that periodic cleaning of the electrode tip surface significantly extended electrode life by improving both variations within each sampling point (weld-to-weld) and throughout the life test. This improvement is obviously due to the prevention of accumulation of Al on the electrode tip surface, as shown in Figure 14, in which EDX measurement of Al was performed on the electrode tip surface before and after cleaning with a 20 weld cleaning interval.

Figures 15 and 16 show the appearances and carbon imprints of electrode surfaces before and after electrode tip life tests, respectively. The new electrode has a smooth tip face with clearly seen tip-face edge. After 2030 welds, the tip face of the electrode without cleaning was completely damaged with a largely increased contact area (Figure 16), but the edge still can be seen. The cleaning every 50 welds clearly delayed the increase in the contact area, which was the reason for the improved tip life (Figure 13), since this would delay the increase in contact area at the faying surface and maintain the current density required for nugget formation. But the electrode with cleaning every 20 welds indicated some alteration of the tip geometry (*e.g.*, part of the tip-face edge was lost, Figure 15(c)). This may be the reason that larger variations occurred in the life test of the electrodes with 20 weld cleaning intervals (after 950 welds, Figure 13), since a distorted electrode surface profile could

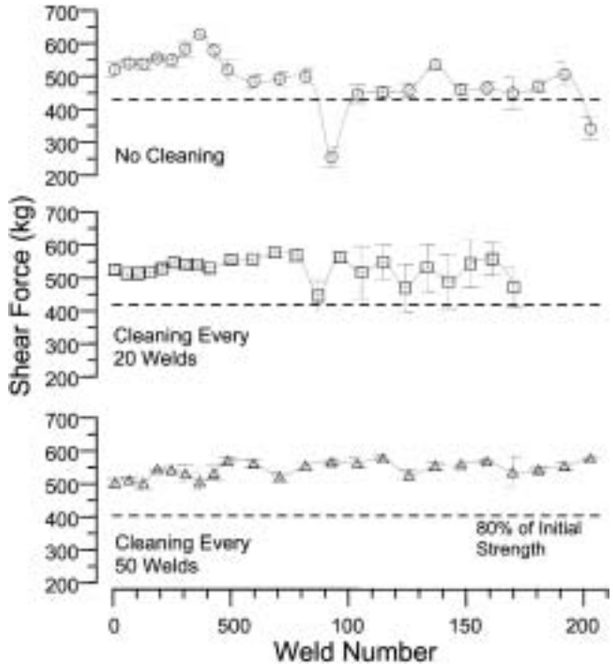

Fig. 13—Effects of electrode cleaning on electrode tip life.

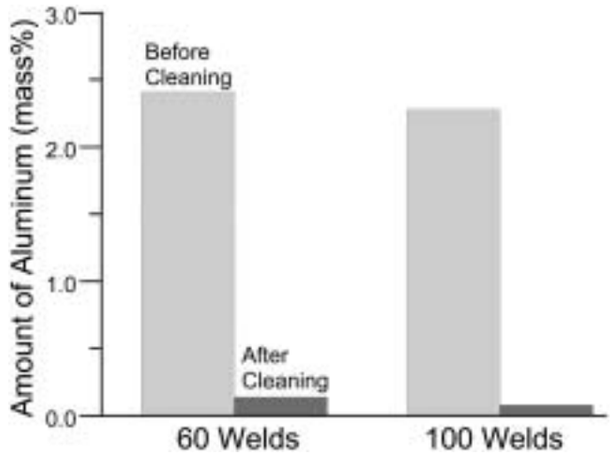

Fig. 14—Aluminum content on the electrode surface before and after cleaning at 20 weld cleaning interval.

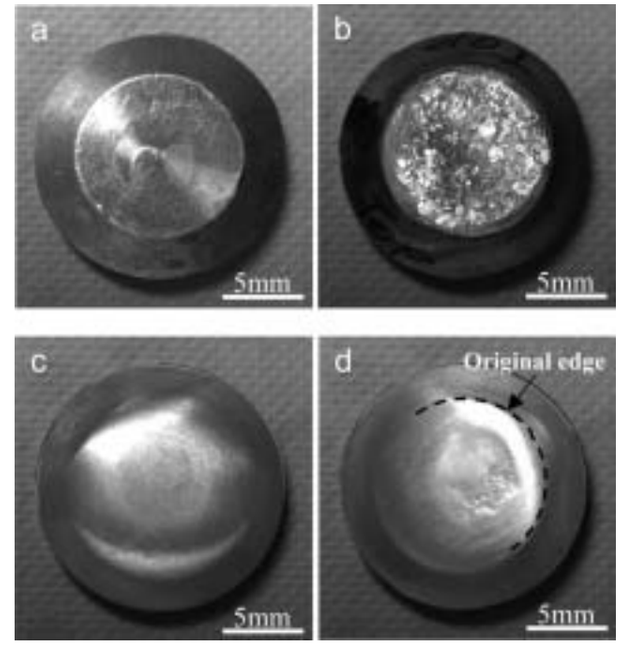

Fig. 15—Surface appearances of (*a*) a new electrode, and used electrodes after 2000 welds; (*b*) without periodic cleaning; (*c*) with cleaning every 20 welds; and (*d*) with cleaning every 50 welds.

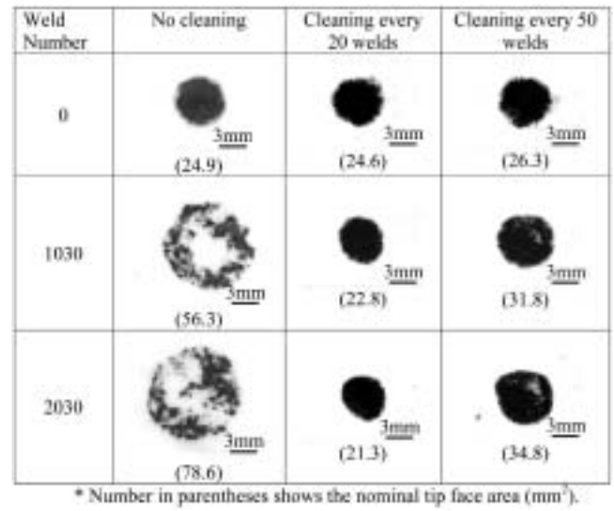

Fig. 16—Carbon imprints of electrodes in electrode life tests with and without cleaning.

affect nugget formation (*e.g.*, by electrode misalignment).[10] This problem could likely be overcome by automated cleaning techniques.

On the other hand, electrode pitting was observed on the carbon imprints after about 1000 welds on the electrode with 50 weld cleaning interval, but not on the electrodes with 20 weld cleaning interval (compared to the incipient pitting at about 120 to 360 welds for electrodes without periodic cleaning). This is because the less frequent cleaning would allow more reaction and alloying of aluminum buildup and larger alloyed regions on the electrodes. For example, the amount of aluminum on the electrode tip surface was approximately 12 mass pct after 50 welds *vs* 1 mass pct after 20 welds (Table III). However, since it is the large cavities not the small pits that cause the electrode to fail (as already discussed previously), the pitting on the electrodes with 50 weld cleaning interval did not result in electrode failure before 2000 welds. It is believed that an optimum cleaning interval may be between 30 and 40 welds.

It is also interesting to note that almost no increase in strength was observed in the beginning of the tip life tests for the electrodes with periodic cleaning (Figure 13). This

confirms that Al pickup and alloying with the electrode tip face was responsible for the initial increase in joint strength[10] because of the higher heat generation due to the higher resistivity of Cu-Al intermetallic compounds.[12] Periodic cleaning would limit the aluminum pickup and alloying with electrode, and hence the increase in contact resistance and heat generation.

IV. SUMMARY

Electrode pitting was investigated in resistance spot welding of 1.5-mm-thick sheet aluminum alloy 5182 using a medium-frequency-direct-current welder and electrodes with a tip face curvature radius of 50 mm and tip face diameter of 10 mm. Detailed investigations of the metallurgical interactions between the copper electrode and aluminum alloy sheet were performed using SEM/EDX and XRD.

The experimental investigations indicated that electrode degradation, which eventually leads to weld failure, could form in four basic steps; aluminum pickup, electrode alloying with aluminum, electrode tip face pitting, and cavitation. Aluminum pickup begins even from the first weld as tiny drops of molten Al alloy are transferred from the sheet surface to the electrode tip face. This molten Al alloy adheres to and reacts with the electrode forming local, complex regions of Cu-Al alloys. The breaking up of the local bonds/alloyed regions, either through transfer of molten Cu-Al mixture or brittle fracture of solidified Cu-Al intermetallic phase(s), would result in electrode pitting, *i.e*., material loss from the tip face. Initial pitting occurs on a ring near the periphery of the contact area and then grows both inward and outward to form large cavities by combining smaller pitted areas. Since pitting and cavitation are results of Al pickup and alloying, periodic electrode cleaning could extend electrode tip life by limiting the buildup of Al on the tip face. Further work is needed to optimize the cleaning intervals.

ACKNOWLEDGMENTS

This study has been supported by the Natural Sciences and Engineering Research Council (NSERC), and the Automobile of the 21st Century (AUTO21), one of the Networks of Centres of Excellence (NCE) programs, both established by the Canadian Government.

REFERENCES

1. R.R. Irving: *Met. Forming*, 2001, Mar., pp. 27-32.
2. J. Matsumoto and H. Mochizuki: *Weld. Int*., 1994, vol. 8 (6), pp. 438-44.
3. T. Saito, Y. Takahashi, and T. Nishi: *Nippon Steel Tech. Rep*., 1988, vol. 37 (4), pp. 24-30.
4. R.M. Rivett and S.A. Westgate: *Met. Constr*., 1980, vol. 12 (10), pp. 510-17.
5. M.A. Glagola and C.A. Roest: SAE Technical Report No. 760167, SAE, Warrendale, PA, 1976.
6. R. Ikeda, K. Yasuda, K. Hashiguchi, T. Okita, and T. Yahaba: *Proc. Advanced Technologies & Processes (IBEC '95)*, SAE, Warrendale, PA, 1995, pp. 144-51.
7. G.L. Leone and B. Altshuller: SAE Technical Paper No. 840292, SAE, Warrendale, PA, 1984.
8. R.M. Rivett: Report No. 132/1980, The Welding Institute, Cambridge, United Kingdom, Dec. 1980.
9. E.P. Patrick and D.J. Spinella: *AWS Sheet Metal Welding Conf*., Detroit Section VII, Troy, MI, Oct. 1996, paper no. 34.
10. I. Lum: Master's Thesis, University of Waterloo, Waterloo, 2002.
11. E.P. Patrick, J.R. Auhl and T.S. Sun: SAE Technical Paper No. 840291, SAE, Warrendale, PA, 1984.
12. U. Dilthey and S. Hicken: *Schweissen and Schneiden*, vol. 50, No.1, 1998, pp. 34-8.
13. *Binary Alloy Phase Diagrams*, T.B. Massalski, ed., ASM INTERNATIONAL, Materials Park, OH, 1990, vol. 1, pp. 141-43.
14. S. Fukumoto, I. Lum, E. Biro, D.R. Boomer, and Y. Zhou: *Welding J*., in press.
15. M. Hasir: *Scheweissen Schneiden*, 1984, vol. 36 (3), pp. 116-21.
16. X.K. Peng, R. Wuhrer, G. Heness, and W.Y. Yeung: *J. Mater. Sci*., 1999, vol. 34 (9), pp. 2029-38.
17. F.A. Calvo, A. Ureña, J.M. Gomez De Salazar, and F. Molleda: *J. Mater. Sci*., 1988, vol. 23 (6), pp. 2273-80.
18. P. Dong, M. Victor Li, and M. Kimchi: *Sci. Technol. Welding Joining*, 1998, vol. 3 (2), pp. 59-64.